IMU Calibration and Validation in a Factory, Remote on Land and at Sea

Martin J. Jørgensen, Dario Paccagnan
and Niels K. Poulsen
Department of Applied Mathemantics and Computer Science
Technical University of Denmark
Kongens Lyngby, Denmark
guuru@dtu.dk, dario.paccagnan@gmail.com, nkpo@dtu.dk

Mikael B. Larsen
Sonardyne International Ltd.
Yateley, United Kingdom
mikael.larsen@sonardyne.com

***Abstract*—This paper treats the IMU calibration and validation problem in three settings: Factory production line with the aid of a precision multi-axis turntable, in-the-field on land and at sea, both without specialist test equipment. The treatment is limited to the IMU calibration parameters of key relevance for gyro-compassing grade optical gyroscopes and force-rebalanced pendulous accelerometers: Scale factor, bias and sensor axes misalignments. Focus is on low-dynamic marine applications e.g., subsea construction and survey.**

Two different methods of calibration are investigated: Kalman smoothing using an Aided Inertial Navigation System (AINS) framework, augmenting the error state Kalman filter (ESKF) to include the full set of IMU calibration parameters and a least squares approach, where the calibration parameters are determined by minimizing the magnitude of the INS error differential equation output.

A method of evaluating calibrations is introduced and discussed. The two calibration methods are evaluated for factory use and results compared to a legacy proprietary method as well as in-field calibration/verification on land and at sea.

The calibration methods shows similar navigation performance as the proprietary method. This validates both methods for factory calibration. Furthermore it is shown that the AINS method can calibrate in-field on land and at sea without the use of a precision multi-axis turntable.

***Keywords*—inertial measurement unit; inertial navigation; sensor fusion; Kalman filters.**

I. Introduction

The core of a strap-down Inertial Navigation System (INS) is an Inertial Measurement Unit (IMU) which is composed of gyroscope and accelerometer triads mounted along nominally orthogonal axes. This paper treats the IMU calibration and validation problem in three substantially different settings:

- Factory production line with the aid of a precision multi-axis turntable.
- On land without specialist test equipment.
- At sea without specialist test equipment.

The treatment is limited to the IMU calibration parameters of key relevance for gyro-compassing grade optical gyroscopes and force-rebalanced pendulous accelerometers: Scale factor, bias and sensor axes misalignments. The latter are determined with respect to precision machined mounting fixtures on the IMU housing enabling easy in the field system replacement. Furthermore, this paper focuses on the low-dynamic marine domain such as subsea survey and construction using Autonomous Underwater Vehicles (AUVs) and Remotely Operated Vehicles (ROVs), and as a supplement to Global Navigation Satellite System (GNSS) to satisfy the redundancy requirements of Dynamic Positioning (DP) drill ships and semi-submersible platforms. Calibration methods for other types of IMU sensor including more complex sensor models for higher dynamics can be found in [1], [2].

The three settings considered are vastly different. Factory calibration using a multi-axis precision turntable benefit from effectively perfect knowledge of absolute orientation, position, (zero) velocity, angular rate and local gravity. Orientation can be controlled arbitrarily to approximately 0.001° accuracy, although some restrictions are imposed if using a dual axis table. Per the nature of the domain, some marine inertial systems are frequently subjected to rough transport, handling and harsh operational conditions. Other systems may be in continuous operation for years. This introduces a special need to reliably validate and calibrate INS performance at customer storage facilities on land or at times offshore. At typical customer sites on land, the reference observation set is limited to fixed position, zero velocity and zero angular rate, relative to Earth. Orientation can be controlled via manual handling and the read-out of the INS itself but no reference is available. At sea the reference observations are severely limited. Approximate position can be provided by GNSS or from knowledge of DP station keeping at a fixed location. Position accuracy is limited by antenna lever arm uncertainty or DP (wave) excursions away from the reference location.

An overview of the different frames used for navigation in this paper is given in section II. Two different methods of calibration are investigated. Both relies on the principle of INS given in section III: Kalman smoothing using a conventional AINS framework, augmenting the ESKF to include the full set of IMU calibration parameters is given in section IV, also investigated in [1]; and a conventional batch least squares optimization approach in section V, where the calibration parameters are determined by minimizing the magnitude of the INS error differential equation output. This technique has

978-1-4799-3320-4/14/$31.00 © 2014 IEEE

been proposed by [3], [4] for similar IMU sensors.

Section VI describes the experimental calibration set-up that forms the basis of the analysis. A method of evaluating calibrations is introduced and discussed in section VII. The two calibration methods are evaluated for factory use and results compared to in-field calibration/verification on land and at sea in section VIII. The calibration trajectory used was chosen to compare a legacy proprietary method with the two presented herein. Alternatively, the trajectory could be chosen as in [3] or even optimized for observability of the estimated parameters as partly examined in [5], [6]. The presented methods are compared and advantages over other methods are discussed in section IX.

II. Reference Frames

The inertial sensor triads gives rise to two non-orthogonal reference frames. Besides the inertial sensor frames the following frames are used in this paper [7]:

- i Inertial frame. Origin is at the center of the Earth with the z-axis coincident with Earth's rotation axis.
- e Earth frame, with origin at the center of the Earth, z-axis coincident with Earth's rotation axis and x-axis through the Greenwich meridian where it intersects the equatorial plane. The e-frame rotates about the z-axis, with respect to the i-frame, at a rate of Ω.
- n North–East–Down (NED) local geographic navigation frame. Rotates with respect to the e-frame with the transport rate, $\boldsymbol{\omega}_{\text{en}}$, which is dependent on motion of the position with respect to Earth.
- b IMU body frame. This is the post-calibrated orthogonal IMU axis set.
- m orientation "sensor" NED local geographic navigation frame. This is not necessarily coincident with the n-frame.

The rotation from b-frame to n-frame can be expressed with the direction cosine matrix (DCM) $\boldsymbol{C}^{\text{n}}_{\text{b}}$. If the DCM is derived from a small angle approximation, also known as the cross-product form, the notation $\boldsymbol{\delta C}^{\text{n}}_{\text{b}} = \boldsymbol{\Psi} = [\boldsymbol{\psi}\times]$, is used, where $\boldsymbol{\psi}$ is the equivalent vector form.

If a vector expressed in b-frame, y^{b}, is to be converted to n-frame, the DCM can be used: $y^{\text{n}} = \boldsymbol{C}^{\text{n}}_{\text{b}} y^{\text{b}}$. This notation is used throughout this paper. Furthermore, the quantity can be explicitly represented e.g., $\boldsymbol{\omega}^{\text{n}}_{\text{en}}$ which means that it is the rotation rate of the e-frame with respect to the n-frame, expressed in n-frame.

III. Inertial Navigation

An INS allows any vehicle to be positioned, in the short term, precisely without having to rely on models of vehicle dynamic. Earth bound navigation using a strap-down IMU can be described with a set of ordinary differential equations (ODEs), derived from the laws of motion within moving coordinate frames. For the chosen n-frame mechanization, the inertial navigation equations (INEs), velocity $\boldsymbol{v}$, position $\boldsymbol{p}$ and orientation $\mathrm{C}^{\text{n}}_{\text{b}}$, can be written as

$$\dot{\boldsymbol{v}}^{\text{n}}_{\text{e}} = [v_{\text{N}}\ v_{\text{E}}\ v_{\text{D}}]^{\top} \tag{1}$$

$$= \underbrace{\mathrm{C}^{\text{n}}_{\text{b}}\boldsymbol{f}^{\text{b}}}_{\text{Inertial}} - \underbrace{(2\boldsymbol{\omega}^{\text{n}}_{\text{ie}} + \boldsymbol{\omega}^{\text{n}}_{\text{en}}) \times \boldsymbol{v}^{\text{n}}_{\text{e}}}_{\text{Coriolis}} + \underbrace{\boldsymbol{g}^{\text{n}}_{\text{l}}}_{\text{Local gravity}} \tag{2}$$

$$\dot{\boldsymbol{p}}^{\text{n}}_{\text{e}} = [L\ \ell\ d]^{\top} \tag{3}$$

$$= \left[\underbrace{\frac{v_{\text{N}}}{R_0 - d}}_{\text{Latitude}}\ \underbrace{\frac{v_{\text{E}}\sec L}{R_0 - d}}_{\text{Longitude}}\ \underbrace{-v_{\text{d}}}_{\text{Height}}\right]^{\top} \tag{4}$$

$$orientation\dot{\mathrm{C}}^{\text{n}}_{\text{b}} = \mathrm{C}^{\text{n}}_{\text{b}}\boldsymbol{\Omega}^{\text{b}}_{\text{nb}}\ , \tag{5}$$

following the notation of [7], with

- $\boldsymbol{f}^{\text{b}}$ specific force as observed by the accelerometers, in m/s^2
- v_{N} local horizontal velocity the in North direction in m/s
- v_{E} local horizontal velocity the in East direction in m/s
- v_{D} vertical velocity in the down direction in m/s
- L latitude in radians
- ℓ longitude in radians
- d depth in meters from mean sea level of the reference ellipsoid
- R_0 radius of the reference ellipsoid at equator, in meters
- $\mathrm{C}^{\text{n}}_{\text{b}}$ platform orientation, DCM from b-frame to n-frame, with the Euler angles $[\alpha\ \beta\ \gamma]^{\top}$
- $\boldsymbol{\Omega}^{\text{b}}_{\text{nb}}$ rotation rate of the n-frame with respect to the b-frame, in rad/s. Calculated from the navigation frame rate $\boldsymbol{\Omega}_{\text{in}}$ and from the absolute body rate $\boldsymbol{\Omega}_{\text{ib}}$ observed by the gyroscopes
- $\boldsymbol{g}^{\text{n}}_{\text{l}}$ local gravity vector, in m/s^2. Often simplified to $[0\ 0\ g]^{\top}$.

The IMU together with the INEs makes up the core of an INS. The INS outputs the *navigation state*; the three dimensional position, attitude, heading, and velocity. Any navigation state can be found by performing dead-reckoning navigation from the previous state. The dead-reckoning navigation can be performed by propagating the IMU measurements through the INEs.

It requires a good initial navigation state for these non-linear equations to work properly, since they are highly dependent on position and orientation. In order to simplify the INS algorithms, the orientation is initialized with an attitude and heading reference system (AHRS). This is a simple, robust and self contained system. The AHRS determines North by use and sensing of the Earths gravitational acceleration and rotation.

Ultimately, the goal of any IMU calibration is to minimize the navigation errors.

IV. AINS framework

Dead-reckoning navigation inhibits poor long term precision performance and will eventually drift off due to sensor errors, modeling errors, initial errors, etc. Errors propagate through

the INEs and build up over time according to the navigation error equations [7], [8]:

$$\dot{\boldsymbol{\delta\psi}} = -\boldsymbol{\omega}^{\mathrm{n}}_{\mathrm{in}} \times \boldsymbol{\psi} + \boldsymbol{\delta\omega}^{\mathrm{n}}_{\mathrm{in}} - \mathrm{C}^{\mathrm{n}}_{\mathrm{b}}\boldsymbol{\delta\omega}^{\mathrm{b}}_{\mathrm{ib}} \tag{6}$$

$$\begin{aligned}\dot{\boldsymbol{\delta v}}^{\mathrm{n}}_{\mathrm{e}} = [\boldsymbol{f}^{\mathrm{n}}\times]\,\boldsymbol{\psi} + \mathrm{C}^{\mathrm{n}}_{\mathrm{b}}\boldsymbol{\delta f}^{\mathrm{b}} - (2\boldsymbol{\omega}^{\mathrm{n}}_{\mathrm{ie}} + \boldsymbol{\omega}^{\mathrm{n}}_{\mathrm{en}}) \times \boldsymbol{\delta v}^{\mathrm{n}}_{\mathrm{e}} \\ - (2\boldsymbol{\delta\omega}^{\mathrm{n}}_{\mathrm{ie}} + \boldsymbol{\delta\omega}^{\mathrm{n}}_{\mathrm{en}}) \times \boldsymbol{v}^{\mathrm{n}}_{\mathrm{e}} - \boldsymbol{\delta g}^{\mathrm{n}}_{\mathrm{l}}\end{aligned} \tag{7}$$

$$\dot{\boldsymbol{\delta p}}^{\mathrm{n}}_{\mathrm{e}} = \boldsymbol{\delta v}^{\mathrm{n}}_{\mathrm{e}} \tag{8}$$

with

$\boldsymbol{\psi}$	platform misalignment vector $[\delta\alpha\ \delta\beta\ \delta\gamma]^\top$
$\boldsymbol{\delta\omega}^{\mathrm{b}}_{\mathrm{ib}}$	gyroscope measurement error
$\boldsymbol{\delta\omega}^{\mathrm{n}}_{\mathrm{ie}}$	error in Earth's spin rate, which is negligible for navigation purposes
$\boldsymbol{\delta f}^{\mathrm{b}}$	accelerometer measurement error
$\boldsymbol{\delta g}^{\mathrm{n}}_{\mathrm{l}}$	error in the local gravity
$\boldsymbol{\delta v}^{\mathrm{n}}_{\mathrm{e}}$	velocity error

where the last three errors are defined similar to (11). These are found e.g., by differencing the estimated INEs and the true INEs.

The complementary properties of extrinsic sensors and the intrinsic can be combined to get the best from both worlds: bounded navigation error with good precision; this is the definition of AINS. An ESKF [7]–[9] framework is used, allowing the estimator to have a slower update rate than the INS, which relaxes requirements for both hardware and algorithms. The states in the ESKF are models of errors, instead of the full states e.g. *estimated depth error* compared to *estimated depth*. Since the INS errors are evolving much slower than the navigational dynamics, it makes sense to make the computational harder estimation task only track the errors. Fig. 1 shows such a processing framework. Aiding sensors make navigation state errors observable. The difference between the expected and the actual observation is fed into the ESKF. The estimated navigational state errors are used as INE corrections. The corrections can be fed back to the INS to let the INS deal with correcting the navigation state. Alternatively the ESKF accumulated corrections can be used to correct the INS navigation state. In the former set-up the ESKF resets the error state vector to zero every time a correction is given to the INS.

An extended Kalman filter (EKF) [9] is employed, as the system is non-linear, here expressed in state-space form

$$\dot{\boldsymbol{x}}(t) = \boldsymbol{f}(\boldsymbol{x}, \boldsymbol{u}_{\mathrm{d}}, t) + \boldsymbol{g}(\boldsymbol{u}, t) \tag{9}$$

$$\boldsymbol{z}(t) = \boldsymbol{h}(\boldsymbol{x}, t) + \boldsymbol{v}(t)\ . \tag{10}$$

The EKF requires knowledge of a nominal state, $\boldsymbol{x}^*$, in order to estimate the true state. The nominal state is defined as being equal to the true state plus an error

$$\boldsymbol{\delta x} = \boldsymbol{x} - \boldsymbol{x}^*. \tag{11}$$

Since the goal is to estimate INS errors, the nominal state is the INS navigation state. Linearizing the system in (9) and (10) with respect to the nominal state gives

$$\dot{\boldsymbol{\delta x}}(t) = \boldsymbol{F}\boldsymbol{\delta x}(t) + \boldsymbol{G}\boldsymbol{u}(t) \tag{12}$$

$$\boldsymbol{\delta z}(t) = \boldsymbol{H}\boldsymbol{\delta x}(t) + \boldsymbol{v}(t), \tag{13}$$

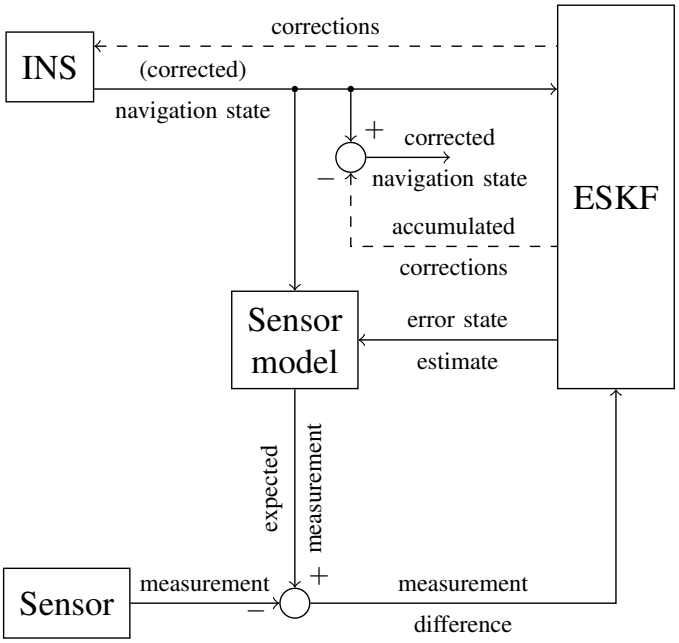

Fig. 1. General AINS framework. The corrections, dashed connections, are either applied to the INS output or alternatively fed back to the INS. If the latter is true, the error state must be reset.

where δ denotes error state and observation error, both from the navigation state, and $\boldsymbol{F}$, $\boldsymbol{G}$ and $\boldsymbol{H}$ are formed from the partial derivatives of $\boldsymbol{f}$, $\boldsymbol{g}$ and $\boldsymbol{h}$, respectively, with respect to $\boldsymbol{x}$; all evaluated in the nominal state. With this linearized system the EKF estimates the error state, $\boldsymbol{\delta\hat{x}}$ and the associated estimation error covariance $\boldsymbol{P}$. it should be emphasized that the EKF should be operating close to the linearization point to minimize non-linear effects.

The resulting parameters are refined by using the Rauch-Tung-Striebel (RTS) fixed interval smoothing technique [9]. For offline processing the RTS interval spans the entire data set, thus making two passes, one forward and one backward. The backward pass is effectively running the KF backwards in time, with the a priori information coming from the forward pass.

A. IMU sensor error models

The ESKF can be used as a parameter estimator for e.g. sensor error models, by augmenting the navigational state-space model:

$$\boldsymbol{\delta x}' = \begin{bmatrix}\boldsymbol{\delta x}_{\mathrm{nav}} \\ \hline \boldsymbol{\delta x}_{\mathrm{sens}}\end{bmatrix} \tag{14}$$

$$\dot{\boldsymbol{\delta x}}'(t) = \boldsymbol{f}'(\boldsymbol{\delta x}'(t)) + \boldsymbol{g}'(\boldsymbol{u}'(t)), \tag{15}$$

where prime, $'$, denotes augmented quantities. Gauss-Markov processes are commonly used for error modeling in ESKFs as they only require a single state, are easy to implement and versatile. A first order Gauss–Markov process, with time-constant τ and variance σ^2, is exponentially-correlated and

can be described by the system

$$x(0) \sim \mathcal{N}(0, \sigma^2) \tag{16}$$

$$\dot{x}(t) = -\frac{1}{\tau}x(t) + \sqrt{\frac{2\sigma^2}{\tau}}u(t), \tag{17}$$

where $u(t)$ is unity white noise . This allows modeling the errors as anything from a random constant, $\tau = \infty$, to almost zero time auto-correlation for $\tau \to 0$ i.e., every sample independently and identically Normal-distributed.

Both the gyroscopes and the accelerometers are modeled as having biases, scale-factor errors and axis misalignment errors, all modeled as first order Gauss–Markov processes. For the calibration problem these are all modeled as random constants. These are applied to the IMU to correct the output with fixed parameters. Unmodeled effects and degradation is accounted for by estimating some or all of the IMU sensor errors as time-varying parameters, when navigating using AINS. These values should be much smaller than the calibrated values for the type of inertial sensors discussed in this article; not necessarily true for other sensor types.

The errors are defined such that the observed quantity ($\widetilde{\ }$) equals the truth plus an error (δ). Thus, the accelerometer model defined as:

$$\widetilde{\boldsymbol{f}}^{\mathrm{b}} = \boldsymbol{f}^{\mathrm{b}} + \boldsymbol{\delta f}^{\mathrm{b}} = \boldsymbol{f}^{\mathrm{b}} + \left(\boldsymbol{\delta f}^{\mathrm{b}}_{\text{bias}} + \boldsymbol{\delta M}_{\mathrm{a}}\boldsymbol{f}^{\mathrm{b}}\right), \tag{18}$$

where $\boldsymbol{f}^{\mathrm{b}}$ is the true specific force in body frame,

$$\boldsymbol{\delta f}^{\mathrm{b}}_{\text{bias}} = \begin{bmatrix} \delta f_{\text{bias,x}} \\ \delta f_{\text{bias,y}} \\ \delta f_{\text{bias,z}} \end{bmatrix} \tag{19}$$

the accelerometer biases with each element modeled with a variance σ^2_{abias} and

$$\boldsymbol{\delta M}_{\mathrm{a}} = \begin{bmatrix} \delta m^{\mathrm{a}}_{11} & \delta m^{\mathrm{a}}_{12} & \delta m^{\mathrm{a}}_{13} \\ \delta m^{\mathrm{a}}_{21} & \delta m^{\mathrm{a}}_{22} & \delta m^{\mathrm{a}}_{23} \\ \delta m^{\mathrm{a}}_{31} & \delta m^{\mathrm{a}}_{32} & \delta m^{\mathrm{a}}_{33} \end{bmatrix}, \tag{20}$$

with the the diagonal elements modeled with the variance σ^2_{asfe} and the off-diagonal elements σ^2_{ama}. Note that $\boldsymbol{\delta M}_{\text{acc}}$ contains both the sensor axes misalignments and the scale-factor errors, which is seen in the structure of the associated variances. Note that this resembles the cross-product form for small angle approximations, but is not quite the same. Also, using this model the diagonal terms will contain a contribution from physical axis misalignments and scale factor errors.

It should be clear that the Gauss–Markov process, (17), only affects its own state in (14). The coupling into the navigation states are found by applying the sensor error model to the navigation error equations. Taking (7) and ignoring products of errors, the tiny contribution from the Coriolis error term and substituting (18) in gives:

$$\boldsymbol{\delta \dot{v}}^{\mathrm{n}}_{\mathrm{e}} = [\boldsymbol{f}^{\mathrm{n}}\times]\,\boldsymbol{\psi} + \mathrm{C}^{\mathrm{n}}_{\mathrm{b}}\boldsymbol{\delta f}^{\mathrm{b}}_{\text{bias}} + \mathrm{C}^{\mathrm{n}}_{\mathrm{b}}\boldsymbol{\delta M}_{\text{acc}}\boldsymbol{f}^{\mathrm{b}} \tag{21}$$

Equation (21) is linearized, when using EKF, to find the couplings in the state transition matrix

$$\begin{aligned}\frac{\partial \boldsymbol{\delta \dot{v}}^{\mathrm{n}}_{\mathrm{e}}}{\partial \boldsymbol{\delta f}^{\mathrm{b}}} &= \frac{\partial \begin{bmatrix} \delta \dot{v}_{\mathrm{N}} & \delta \dot{v}_{\mathrm{E}} & \delta \dot{v}_{\mathrm{D}} \end{bmatrix}^{\top}}{\partial \begin{bmatrix} \delta f_{\text{bias,x}} & \delta f_{\text{bias,y}} & \delta f_{\text{bias,z}} & \delta m^{\mathrm{a}}_{11} & \cdots & \delta m^{\mathrm{a}}_{33} \end{bmatrix}^{\top}} \\ &= \mathrm{C}^{\mathrm{n}}_{\mathrm{b}} \begin{bmatrix} \mathbf{I_3} & \mathbf{I_3} f_x & \mathbf{I_3} f_y & \mathbf{I_3} f_z \end{bmatrix},\end{aligned} \tag{22}$$

where $\mathbf{I_3}$ is the 3x3 identity matrix.

Similarly, the gyroscope sensor model is defined:

$$\widetilde{\boldsymbol{\omega}}^{\mathrm{b}}_{\mathrm{ib}} = \boldsymbol{\omega}^{\mathrm{b}}_{\mathrm{ib}} + \boldsymbol{\delta\omega}^{\mathrm{b}}_{\mathrm{ib}} = \boldsymbol{\omega}^{\mathrm{b}}_{\mathrm{ib}} + \left(\boldsymbol{\delta\omega}^{\mathrm{b}}_{\text{ib,bias}} + \boldsymbol{\delta M}_{\mathrm{g}}\boldsymbol{\omega}^{\mathrm{b}}_{\mathrm{ib}}\right), \tag{23}$$

with $\boldsymbol{\omega}^{\mathrm{b}}_{\mathrm{ib}}$ being the true angular velocity of the body frame with respect to the inertial frame, expressed in body frame,

$$\boldsymbol{\delta\omega}^{\mathrm{b}}_{\text{ib,bias}} = \begin{bmatrix} \delta\omega_{\text{bias,x}} \\ \delta\omega_{\text{bias,y}} \\ \delta\omega_{\text{bias,z}} \end{bmatrix} \tag{24}$$

the gyroscope biases with each element modeled with a variance σ^2_{gbias} and

$$\boldsymbol{\delta M}_{\mathrm{g}} = \begin{bmatrix} \delta m^{\mathrm{g}}_{11} & \delta m^{\mathrm{g}}_{12} & \delta m^{\mathrm{g}}_{13} \\ \delta m^{\mathrm{g}}_{21} & \delta m^{\mathrm{g}}_{22} & \delta m^{\mathrm{g}}_{23} \\ \delta m^{\mathrm{g}}_{31} & \delta m^{\mathrm{g}}_{32} & \delta m^{\mathrm{g}}_{33} \end{bmatrix}, \tag{25}$$

with the the diagonal elements modeled with the variance σ^2_{gsfe} and the off-diagonal elements σ^2_{gma}. Taking (6) and ignoring products of errors and substituting with (23)

$$\boldsymbol{\delta\dot{\psi}} = -\boldsymbol{\omega}^{\mathrm{n}}_{\mathrm{in}} \times \boldsymbol{\psi} + \boldsymbol{\delta\omega}^{\mathrm{n}}_{\mathrm{in}} - \mathrm{C}^{\mathrm{n}}_{\mathrm{b}}\boldsymbol{\delta\omega}^{\mathrm{b}}_{\text{ib,bias}} - \mathrm{C}^{\mathrm{n}}_{\mathrm{b}}\boldsymbol{\delta M}_{\mathrm{g}}\boldsymbol{\omega}^{\mathrm{b}}_{\mathrm{ib}}, \tag{26}$$

yields the system combined equation. Again, the gyroscope error states influence on the navigation states are found by linearizing (26):

$$\begin{aligned}\frac{\partial \boldsymbol{\delta\dot{\psi}}}{\partial \boldsymbol{\delta\omega}^{\mathrm{b}}_{\mathrm{ib}}} &= \frac{\partial \begin{bmatrix} \delta\dot{\alpha} & \delta\dot{\beta} & \delta\dot{\gamma} \end{bmatrix}^{\top}}{\partial \begin{bmatrix} \delta\omega_{\text{bias,x}} & \delta\omega_{\text{bias,y}} & \delta\omega_{\text{bias,z}} & \delta m^{\mathrm{g}}_{11} & \cdots & \delta m^{\mathrm{g}}_{33} \end{bmatrix}^{\top}} \\ &= -\mathrm{C}^{\mathrm{n}}_{\mathrm{b}} \begin{bmatrix} \mathbf{I_3} & \mathbf{I_3}\omega^{\mathrm{b}}_{\text{ib,x}} & \mathbf{I_3}\omega^{\mathrm{b}}_{\text{ib,y}} & \mathbf{I_3}\omega^{\mathrm{b}}_{\text{ib,z}} \end{bmatrix},\end{aligned} \tag{27}$$

where $\mathbf{I_3}$ is the 3x3 identity matrix. The similarity between (22) and (27) is expected since the sensor models are identical and as both couple sensor errors into identical state dynamic, i.e., accelerometer to velocity and gyroscope to angular velocity.

B. Factory observations

The AINS is initialized with knowledge of the absolute orientation and position. Knowledge of local gravity is used to adjust the depth, so it fits with the reference frame, WGS-84 in this case.

Whenever stationary the AINS is aided by orientation from the turn table, mean depth and zero velocity. The two latter are pseudo sensors. They provide aiding information, but relies on the operator to satisfy/verify the assumptions. In case these assumptions does not hold true and the aiding is enabled, the ESKF will be provided with wrongful information that "can not escape". So once the information is there it will flow to the least observable states, leading to estimation errors perhaps even loss of integrity i.e., when the true estimation error is not consistent with the propagated covariance.

1) Orientation: An orientation sensor observes the body frame orientation with respect to the orientation sensor local navigation frame, that is $\mathrm{C}_{\mathrm{b}}^{\mathrm{m}}$. The actual orientation observation is taken from the reference platform, the two-axis turntable, although the following mechanization is general in nature.

$$\widetilde{\mathrm{C}}_{\mathrm{b}}^{\mathrm{m}} = \left[\begin{bmatrix} \alpha_{\text{att}} \\ \beta_{\text{att}} \\ \gamma_{\text{att}} \end{bmatrix} \times \right] + w_{\text{att}}, \tag{28}$$

where $w_{\text{att}} \sim \mathcal{N}(\mathbf{0}, \mathrm{I}_3 \sigma_{\text{att}})$. The related expected observation is given by

$$\widehat{\mathrm{C}}_{\mathrm{b}}^{\mathrm{m}} = \widehat{\mathrm{C}}_{\mathrm{n}}^{\mathrm{m}} \widehat{\mathrm{C}}_{\mathrm{b}}^{\mathrm{n}}. \tag{29}$$

The estimated navigation frame orientation with respect to the orientation sensor local navigation frame is defined as

$$\widehat{\mathrm{C}}_{\mathrm{n}}^{\mathrm{m}} = \left[\mathrm{I}_3 - \boldsymbol{\Sigma}\right] \mathrm{C}_{\mathrm{n}}^{\mathrm{m}}, \tag{30}$$

where $\boldsymbol{\Sigma} = [\boldsymbol{\varsigma}\times]$ and

$$\boldsymbol{\varsigma} = \begin{bmatrix} \delta\alpha_{\text{att}} \\ \delta\beta_{\text{att}} \\ \delta\gamma_{\text{att}} \end{bmatrix} \tag{31}$$

are small misalignment angles modeled as Gauss–Markov processes with variance σ_{att}^2. The ESKF observation is modeled as the small misalignment angles between the estimated and observed orientation,

$$\boldsymbol{\delta}\mathrm{C}_{\mathrm{n}}^{\mathrm{m}} = \mathrm{I}_3 - \widehat{\mathrm{C}}_{\mathrm{b}}^{\mathrm{m}} \mathrm{C}_{\mathrm{b}}^{\mathrm{m}\top}, \tag{32}$$

which comes from the definition of orientation errors i.e., same as (30). Expanding and ignoring products of errors

$$\begin{aligned} \boldsymbol{\delta}\mathrm{C}_{\mathrm{n}}^{\mathrm{m}} &= \mathrm{I}_3 - \widehat{\mathrm{C}}_{\mathrm{n}}^{\mathrm{m}} \widehat{\mathrm{C}}_{\mathrm{b}}^{\mathrm{n}} \mathrm{C}_{\mathrm{b}}^{\mathrm{m}\top} \\ &= \mathrm{I}_3 - \left[\mathrm{I}_3 - \boldsymbol{\Sigma}\right] \mathrm{C}_{\mathrm{n}}^{\mathrm{m}} \left[\mathrm{I}_3 - \boldsymbol{\Psi}\right] \mathrm{C}_{\mathrm{b}}^{\mathrm{n}} \mathrm{C}_{\mathrm{b}}^{\mathrm{m}\top} \\ &\approx \mathrm{C}_{\mathrm{n}}^{\mathrm{m}} \boldsymbol{\Psi} \mathrm{C}_{\mathrm{n}}^{\mathrm{m}\top} + \boldsymbol{\Sigma} \end{aligned} \tag{33}$$

or on vector form

$$\boldsymbol{\delta\xi} = \mathrm{C}_{\mathrm{n}}^{\mathrm{m}} \boldsymbol{\psi} + \boldsymbol{\varsigma}, \tag{34}$$

where $\boldsymbol{\delta\xi}$ is the misalignment angles corresponding to the DCM $\boldsymbol{\delta}\mathrm{C}_{\mathrm{n}}^{\mathrm{m}}$. The corresponding observation matrix is found by linearizing (34),

$$\boldsymbol{H}(\boldsymbol{\psi}, \boldsymbol{\varsigma}) = \frac{\partial \boldsymbol{\delta\xi}}{\partial \boldsymbol{\delta x}} = \begin{bmatrix} \mathrm{C}_{\mathrm{n}}^{\mathrm{m}} & \mathrm{I}_3 \end{bmatrix}, \tag{35}$$

which is trivial in this case.

2) Zero velocity: If completely stationary an observation of zero velocity, relative to Earth, is a rather good approximation. This is also known as zero velocity update (ZUPT). The observed zero velocity is simply

$$\tilde{\boldsymbol{v}}^{\mathrm{n}} = \mathbf{0}, \tag{36}$$

and the expected observation

$$\hat{\boldsymbol{v}}^{\mathrm{n}} = \mathbf{0} + \boldsymbol{\delta v}^{\mathrm{n}}, \tag{37}$$

with $\boldsymbol{\delta v}^{\mathrm{n}}$ modeled as with a variance of σ_{zupt}^2. The observable difference is simply

$$\begin{aligned} \boldsymbol{\delta v}^{\mathrm{n}} &= \hat{\boldsymbol{v}}^{\mathrm{n}} - \tilde{\boldsymbol{v}}^{\mathrm{n}} \\ &= (\mathbf{0} + \boldsymbol{\delta v}^{\mathrm{n}}) - \mathbf{0} \\ &= \boldsymbol{\delta v}^{\mathrm{n}} \end{aligned} \tag{38}$$

and the observation matrix

$$\boldsymbol{H}(\boldsymbol{\delta v}^{\mathrm{n}}) = \frac{\partial \boldsymbol{\delta v}^{\mathrm{n}}}{\partial \boldsymbol{\delta x}} = \mathrm{I}_3. \tag{39}$$

As seen from (38) and (39) the ESKF estimate is directly the estimation error, with corresponding noise.

3) Mean depth: With ZUPT aiding the position drift of the AINS is minimized, but the vertical channel is unstable [7], [8] will diverge if not aided. Using the same principle as with ZUPT, the observed depth is

$$\tilde{d} \sim \mathcal{N}(d_0, \sigma_{\mathrm{d}}), \tag{40}$$

where d_0 is the constant depth found from the local gravity. With the expected observation

$$\hat{d} = d_0 + \delta d, \tag{41}$$

the observable difference is found

$$\begin{aligned} \delta d &= \hat{d} - \tilde{d} \\ &= (d_0 + \delta d) - d_0. \\ &= \delta d \end{aligned} \tag{42}$$

The observation matrix is simply

$$\boldsymbol{H}(\delta d) = \frac{\partial \delta d}{\partial \boldsymbol{\delta x}} = 1. \tag{43}$$

The final augmented system consists of 36 states: 9 navigation error states, 24 IMU sensor error states and 3 orientation sensor platform misalignment states.

C. On land

Even without orientation observations, the AINS described in the previous section will be able to calibrate the IMU, but the lacking orientation information makes the IMU housing orientation unobservable and thus indeterminable.

A gravity model must be used, as it is unlikely that the remote site has surveyed local gravity. In order to achieve good estimates for the accelerometer scale-factor errors, a gravity model accounting for the spherical harmonics must be employed. Such models are readily available in public domain. For navigational performance an error in the order of deci-micro-g is insignificant and the models should suffice.

The AINS is initialized with orientation from the AHRS and position from an approximately known fixed position and aided with ZUPT and mean depth. Constant orientation aiding using the knowledge of rotational stationarity, much like ZUPT, is believed to increase observability of the calibration parameters, but is not being investigated in this paper.

The final augmented system consists of 33 states: 9 navigation error states, 24 IMU sensor error states.

D. At sea

The only partly known quantities are the horizontal position, and mean depth equal to roughly the mean sea level. The latter is derived in section IV-B3.

The position is aided by a GNSS. These vessels tend to place the GNSS receiver as high as possible, operationally resulting in a large sensor lever arm. Errors will be introduced if the lever arm is incorrectly compensated for e.g., erroneous surveyed, if the vessel is unstable.

1) Position: Using the same principle as with ZUPT, the observed position is

$$\widetilde{\boldsymbol{p}} = \boldsymbol{p} = \begin{bmatrix} p_{\text{lat}} \\ p_{\text{lon}} \end{bmatrix} \tag{44}$$

where $\boldsymbol{p}$ is the true position. With the expected observation

$$\widehat{\boldsymbol{p}} = \boldsymbol{p} + \boldsymbol{\delta p}, \tag{45}$$

where δp_{lat} is modeled with a variance σ^2_{lat} and δp_{lon} with σ^2_{lon}. The observable difference is derived:

$$\begin{aligned} \boldsymbol{\delta p} &= \widehat{\boldsymbol{p}} - \widetilde{\boldsymbol{p}} \\ &= (\boldsymbol{p} + \boldsymbol{\delta p}) - \boldsymbol{p} \\ &= \boldsymbol{\delta p} \end{aligned} \tag{46}$$

The observation matrix is simply

$$\boldsymbol{H}(\boldsymbol{\delta p}) = \frac{\partial \boldsymbol{\delta p}}{\partial \boldsymbol{\delta x}} = \mathrm{I}_2. \tag{47}$$

The final augmented system consists of 33 states: 9 navigation error states, 24 IMU sensor error states.

V. Batch/least squares processing

The fundamental idea behind the least-squares calibration method is adjusting the calibration parameter such that the error of the INEs is minimized rather than directly comparing the IMU sensor output with a computed reference. This technique has the advantage of being robust with respect to errors in the experimental setup. Furthermore, it does not require elaborate IMU sensor noise models unlike the AINS method. The measurable difference in acceleration error for two different IMU orientations is a function of the calibration parameters, as seen from (6) and (7). If the rotations are carefully chosen, the full set of parameters is observable. In the simplest case, this yields an algebraic system of equations, which can be solved using a least-squares technique [10]. Alternatively, a larger and more complex set of rotations can be chosen e.g., optimized for observability, and the parameters estimated using optimization. Both approaches assumes that the IMU is stationary relative to Earth, at the start, T_0, and end, T, of each rotation, which greatly simplifies (7). Thus, the i'th residual $\boldsymbol{r}_i$ can be written as

$$\boldsymbol{r}_i = \underbrace{\boldsymbol{C}^{\text{n}}_{\text{b}}(T_{0,i})}_{\text{table}} \underbrace{\widetilde{\boldsymbol{f}}^{\text{b}}(T_{0,i})}_{\text{acc.}} - \underbrace{\widehat{\boldsymbol{C}}^{\text{n}}_{\text{b}}(T_i)}_{\text{gyro.}} \underbrace{\widetilde{\boldsymbol{f}}^{\text{b}}(T_i)}_{\text{acc.}}, \tag{48}$$

where $\widetilde{\boldsymbol{f}}^{\text{b}}$ are accelerometer measurements, $\boldsymbol{C}^{\text{n}}_{\text{b}}(T_{0,i})$ is the absolute orientation from the turn table at the beginning of the rotation and $\widehat{\boldsymbol{C}}^{\text{n}}_{\text{b}}(T_i)$ the INS estimated orientation at the end of the rotation. The IMU measurements are compensated applying current parameter estimates before any calculations. The gyroscope sensor errors will propagate through the estimated orientation in (48), making all IMU sensor errors observable in the residual.

The optimization problem for the calibration parameter set $\boldsymbol{\theta}$ is then formulated as:

$$\arg\min_{\boldsymbol{\theta}} \|\boldsymbol{r}\|_2^2 \ , \tag{49}$$

and solved using classical nonlinear least squares techniques. Note that the minimization of the residuals defined in (48) only guarantees internal consistency of the IMU data, but does not estimate the IMU sensor orientation with respect to a predetermined external frame of reference e.g., the IMU housing. If the value of the gravity vector $\boldsymbol{g}$ is known with sufficient precision, then minimizing the (new) residuals

$$\tilde{\boldsymbol{r}}_i = \begin{bmatrix} \boldsymbol{C}^{\text{n}}_{\text{b}}(T_{0,i})\widetilde{\boldsymbol{f}}^{\text{b}}(T_{0,i}) - \boldsymbol{g}^{\text{n}} \\ \widehat{\boldsymbol{C}}^{\text{n}}_{\text{b}}(T_{\infty,i})\widetilde{\boldsymbol{f}}^{\text{b}}(T_{\infty,i}) - \boldsymbol{g}^{\text{n}} \end{bmatrix} \ , \tag{50}$$

allows also to determine the orientation of the sensors with respect to the table frame of reference.

The least-squares approach is only used for the factory setting. Major rework would be necessary to make it work for the other settings, as it is not as easily reconfigured for different observations as the AINS.

VI. Calibration set-up

The basis of the calibration is experimental data from six IMUs on a two-axis turn table. The pre-calibrated 100 Hz IMU data is collected after the coning and sculling algorithm [7], [8] is applied. The IMUs are undergoing a rotation sequence similar to that in Fig. 2. This sequence of rotations can be realized in all three settings, either by hand or with help of a fixture. Having the reference data from the table serves as a mean to evaluate the calibration methods in all settings.

For the factory setting the table orientation is available for the calibration methods, as well as surveyed local gravity. Both the AINS and the least-squares methods are compared to a third proprietary calibration method. This method does not determine the IMU sensor orientation with respect to the IMU housing, but it does ensure an orthogonal calibrated body frame.

Note that the processing for the on land and at sea settings does not require the IMU to follow the referenced example trajectory absolutely, as only the stationary periods matter.

Using the data sets for the at sea setting is justified by the fact that large vessels with DP systems in calm waters have negligible attitude motion, thus any GNSS lever arm errors will have no influence. GNSS observations are simulated by taking the table position and adding 30 cm white noise.

Gyroscope biases are not calibrated for all methods and all settings, due to small biases for the available IMUs.

All calibration methods output the calibration parameter set and produces pertaining compensated IMU data.

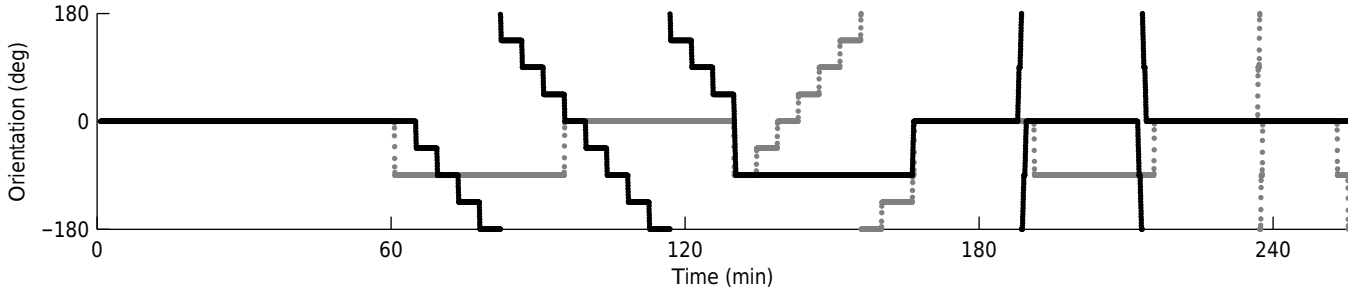

Fig. 2. Calibration fixture, two-axis turn table, example rotation sequence. Black is the inner axis and gray the outer axis.

VII. Evaluation

Evaluating the navigational performance of IMU calibrations is non-trivial due to different definitions of e.g., calibrated body frame. A calibration should be penalized if the calibrated body frame is non-orthogonal, but not if it is not calibrated to IMU housing frame. An evaluation method using calibrated IMU data is presented in this section.

Two metrics are evaluated: the navigation frame misalignment and the acceleration error in navigation frame. Evaluating errors in navigation frame makes comparison easier than dealing with different definitions of body frame. The references are the IMU motion from the calibration platform and the surveyed gravity, respectively.

The IMU body frame orientation with respect to the navigation frame, $\boldsymbol{C}_{\mathrm{b}}^{\mathrm{n}}[t]$, is found by running ZUPT aided INS. The initial orientation and position are taken from the reference platform. The body frames of the platform and the IMU might not be perfectly aligned. Additionally the available calibration fixture had a small but unknown heading misalignment. Consequently the platform orientation reference, $\boldsymbol{C}_{\mathrm{bp}}^{\mathrm{np}}[t]$, can not be directly compared to $\boldsymbol{C}_{\mathrm{b}}^{\mathrm{n}}[t]$. These misalignments are small and constant throughout the entire procedure, and are fitted with the residuals

$$\boldsymbol{r}_{\mathrm{att}}[t] = \boldsymbol{C}_{\mathrm{b}}^{\mathrm{n}}[t] \left[\boldsymbol{C}_{\mathrm{np}}^{\mathrm{n}}(\gamma_{\mathrm{np}}) \boldsymbol{C}_{\mathrm{bp}}^{\mathrm{np}}[t] \boldsymbol{C}_{\mathrm{b}}^{\mathrm{bp}}(\theta_{\mathrm{bp}}) \right]^{\top}, \tag{51}$$

where the Euler angle γ_{np} is the heading difference and $\theta_{\mathrm{bp}} = \begin{bmatrix} \alpha_{\mathrm{bp}} & \beta_{\mathrm{bp}} & \gamma_{\mathrm{bp}} \end{bmatrix}^{\top}$ the body frame misalignments. The minimization problem

$$\underset{\{\gamma_{\mathrm{np}}, \theta_{\mathrm{bp}}\}}{\arg\min} \left\| \boldsymbol{j}(\boldsymbol{r}_{\mathrm{att}}) \right\|_2^2, \tag{52}$$

with function $\boldsymbol{j}$ resolving the residuals into Euler angles and taking the 2-norm of the three Euler elements, is solved by a conventional non-linear least-squares algorithm. Running the AINS as part of the minimization increases the execution time immensely, as a result a slightly different approach is used. Running the AINS with an initial heading error will converge with time, so using RTS smoothing on the result gives an improved initial heading. This mitigates the initial heading error effect on the AINS and the optimization executes fast. The appertaining root–mean–square–error (RMSE) is calculated as the RMS of the minimized residuals of (51), for stationary periods.

The navigation frame acceleration error is evaluated by resolving the body frame output of the accelerometers, $\boldsymbol{\Delta v}^{\mathrm{b}}$, into navigation frame using the gyroscopes

$$\boldsymbol{\Delta v}^{\mathrm{n}}[t] = \boldsymbol{C}_{\mathrm{b}}^{\mathrm{n}}[t] \boldsymbol{\Delta v}^{\mathrm{b}}[t], \tag{53}$$

and compensated for gravity

$$\boldsymbol{\delta a}^{\mathrm{n}}[t] = \frac{\boldsymbol{\Delta v}^{\mathrm{n}}[t]}{\Delta T_{\mathrm{IMU}}} - \begin{bmatrix} 0 \\ 0 \\ g \end{bmatrix}, \tag{54}$$

where ΔT_{IMU} is the IMU sample interval. Taking the RMSE of the magnitude of the acceleration will unfairly weight longer stationary periods more than shorter periods. Both problems are mitigated by taking the mean of $\boldsymbol{\Delta v}^{\mathrm{n}}$ for each stationary period, weighting each period equally, before calculating the RMSE.

VIII. Results

The calibration methods are evaluated according to the metrics defined in section VII, using the set-up described in section VI.

Table I and II shows orientation and acceleration performance, respectively, for the factory calibration setting. In this setting the two calibration methods described in this paper has been verified against a third proprietary calibration method. Calibration performance for the on land setting is shown in table III and at sea in table IV.

Comparing the results shows that all three methods perform similarly for the factory setting. Furthermore, it is also seen that the performance of the AINS method performs almost identically in all three settings.

IX. Conclusion

Analyzing the results from the experimental data shows that both methods presented herein can be used to achieve high accuracy for factory calibration. Furthermore, utilizing two substantially different algorithms is a useful aid in validation of correctness of implementation. Both algorithms are found to perform on par or better than a proprietary and previously used method.

In-the-field calibration on land is shown to be feasible without a multi axis precision turn table, by merely doing a nominally similar series of rotations and leaving the IMU stationary in-between and making use of the flexibility of

TABLE I
ATTITUDE AND HEADING PERFORMANCE FOR FACTORY SETTING.

	Orientation RMSE (mili-$^\circ$)		
IMU#	AINS	NLSQ	Proprietary
1	10.7668	11.0004	12.8470
2	20.3281	20.9816	21.9415
3	26.6626	26.1676	27.4034
4	22.3295	23.0129	22.6769
5	28.8444	27.5539	25.1533
6	26.3689	26.5847	26.5428
Mean	22.5500	22.5502	22.7608

TABLE II
ACCELERATION PERFORMANCE FOR FACTORY SETTING.

	Acceleration RMSE (μg)		
IMU#	AINS	NLSQ	Proprietary
1	16.7683	16.4582	21.9174
2	29.9454	26.5149	29.7009
3	28.5088	22.1025	89.6507
4	33.2744	29.1359	28.2366
5	25.6030	23.4516	31.6360
6	31.9135	30.0562	34.0508
Mean	27.6689	24.6199	39.1987

the AINS KF. Without absolute knowledge of orientation, calibration to the IMU housing is unattainable.

In-field calibration at sea is shown feasible if certain conditions are met. Results shows that the IMU can be field calibrated with just a GNSS receiver and knowledge of local gravity or a good model hereof.

Compared to the least-squares method, the AINS KF approach benefits from the ESKFs ability to process a wide range of external observations. The framework's flexibility allows easy adaptation to the available set of observations for each of the settings. Using the KF covariance matrix to evaluating parameter observability/accuracy and optimizing the sequence of rotations might increase calibration accuracy. A drawback of applying the AINS Kalman filter technique is dependence on accurate IMU sensor noise models. A disadvantage that the least-squares method does not share.

Finally, an evaluation method has been developed that allows for a robust comparison of IMU performance.

TABLE III
CALIBRATION PERFORMANCE FOR ON LAND SETTING.

	RMSE	
IMU#	Orientation (mili-$^\circ$)	Acceleration (μg)
1	30.1818	67.6954
2	20.4200	29.8001
3	26.4714	26.8985
4	22.9644	27.8462
5	28.0645	28.9807
6	25.4839	29.7186
Mean	25.5977	35.1566

TABLE IV
CALIBRATION PERFORMANCE FOR AT SEA SETTING.

	RMSE	
IMU#	Orientation (mili-$^\circ$)	Acceleration (μg)
1	17.6468	28.5954
2	20.0357	32.6557
3	25.8094	34.5786
4	25.2287	31.4044
5	27.4300	24.9405
6	27.9529	33.9529
Mean	24.0173	31.0213

REFERENCES

[1] M. Grewal, V. Henderson, and R. Miyasako, "Application of Kalman filtering to the calibration and alignment of inertial navigation systems," *IEEE Transactions on Automatic Control*, vol. 36, no. 1, pp. 3–13, 1991.

[2] D. Joos and U. Krogmann, "Estimation of strapdown sensor parameters for inertial system error-compensation," ... *Precision Positioning and Inertial Guidance Sensors* ..., 1981.

[3] J. DIESEL, "Calibration of a ring laser gyro inertial navigation system," *Test Group(6585 th), 13 th Biennial Guidance Test* ..., vol. I, 1987.

[4] A. Brown, R. Ebner, and J. Mark, "A Calibration Technique for a Laser Gyro Strapdown Inertial Navigation System," *SYMPOSIUM GYRO TECHNOLOGY 1982 conference proceedings*, pp. 12–12.20, 1982.

[5] M. Grewal, "Optimal selection of trajectories for parameter estimation in dynamical systems," in *1982 21st IEEE Conference on Decision and Control*, vol. 21. IEEE, 1982, pp. 1140–1141.

[6] L. J. Lintereur, "Optimal Test Trajectories for Calibrating Inertial Systems," Ph.D. dissertation, Massachusetts Institute of Technology, 1996.

[7] D. Titterton, *Strapdown Inertial Navigation Technology, 2nd Edition*. IET, 2004.

[8] P. D. Groves, *Principles of GNSS, Inertial, and Multisensor Integrated Navigation Systems, Second Edition*. Artech House, 2013.

[9] R. G. Brown and P. Y. C. Hwang, *Introduction to Random Signals and Applied Kalman Filtering*, 3rd ed. Wiley, 1996.

[10] R. Rogers, "Applied mathematics in integrated navigation systems," *AIAA Education series*, 2003.